

## QUANTITATIVE STRUCTURE-METABOLISM RELATIONSHIP MODELING OF METABOLIC *N*-DEALKYLATION REACTION RATES

Konstantin V. Balakin, Sean Ekins, Andrey Bugrim, Yan A. Ivanenkov, Dmitry Korolev, Yuri V. Nikolsky, Andrey A. Ivashchenko, Nikolay P. Savchuk, and Tatiana Nikolskaya

*Chemical Diversity Labs, Inc., San Diego, California. (K.V.B., Y.A.I., D.K., A.A.I., N.P.S.); and GeneGo, Inc., St. Joseph, Michigan (S.E., A.B., Y.V.N., T.N.)*

Received April 21, 2004; accepted July 12, 2004

### ABSTRACT:

It is widely recognized that preclinical drug discovery can be improved via the parallel assessment of bioactivity, absorption, distribution, metabolism, excretion, and toxicity properties of molecules. High-throughput computational methods may enable such assessment at the earliest, least expensive discovery stages, such as during screening compound libraries and the hit-to-lead process. As an attempt to predict drug metabolism and toxicity, we have developed an approach for evaluation of the rate of *N*-dealkylation mediated by two of the most important human cytochrome P450s (P450), namely CYP3A4 and CYP2D6. We have taken a novel approach by using descriptors generated for the whole molecule, the reaction centroid, and the leaving group, and then applying neural network computations and sensitivity analysis to

generate quantitative structure-metabolism relationship models. The quality of these models was assessed by using the cross-validated correlation coefficients of 0.82 for CYP3A4 and 0.79 for CYP2D6 as well as external test molecules for each enzyme. The relative performance of different neural networks was also compared, and modular neural networks with two hidden layers provided the best predictive ability. Functional dependencies between the neural network input and output variables, generalization ability, and limitations of the described approach are also discussed. These models represent an initial approach to predicting the rate of P450-mediated metabolism and may be applied and integrated with other models for P450 binding to produce a systems-based approach for predicting drug metabolism.

Quantitative structure-metabolism relationship (QSMR) models allow the estimation of complex metabolism-related phenomena from relatively simple calculated molecular properties or descriptors. Such models can be used for the design of structural analogs of bioactive compounds with improved pharmacokinetic properties (Bouska et al., 1997; Madsen et al., 2002; Humphreys et al., 2003), evaluation of excretion kinetics (Holmes et al., 1995; Bollard et al., 1996; Cupid et al., 1996), estimation of approximate rates of metabolic conversion for prodrugs or soft drug candidates (Buchwald and Bodor, 1999; Bodor, 1999), and assessment of potential toxic effects of novel compounds. (Di Carlo et al., 1986a,b; Di Carlo, 1990; Altomare et al., 1992).

The computational prediction of the metabolic fate of novel compounds is a nontrivial problem. First, an indiscriminate pooling of metabolic data from different species in the commercially available databases substantially distorts any attempt at generalization (Darvas, 1988). The metabolic pathways and corresponding networks can be very different even in close mammalian species, so that any use of such pooled data is problematic (Mulder, 1990). Second, *in vitro* and *in vivo* data may differ substantially even for the same species. The metabolic fate of a drug delivered to the human liver after intravenous administration is often quite different from that observed in the liver

microsomal fraction *in vitro*. Third, metabolism of the same drug may vary substantially between individuals depending on the expression level of particular enzymes, polymorphisms in enzyme-encoding and regulatory genes, and the presence of particular isoenzymes in normal (Hayashi et al., 1991) and disease states (Kato et al., 1995). In determining a QSMR, the key question is whether it is the complete molecular structure or its structural components that actually undergo metabolism. The answer is vital for choosing relevant descriptors for QSMR models and the subsequent prediction of metabolic fate for novel compounds. Finally, such QSMR algorithms should be highly effective in handling very large virtual and real discovery compound databases.

We have applied QSMR to the cytochrome P450 (P450) enzymes involved in the phase I metabolism of both exogenous and endogenous compounds (Ioannides and Parke, 1996). The recent reviews on P450s detail their chemistry, regulation, membrane topology, and molecular biology, and provide initial models for substrate-binding sites (Ioannides and Parke, 1996; Ekins et al., 2003). Of over 50 human P450 genes cloned and described, only three P450 families, a half-dozen subfamilies, and fewer than a dozen isoenzymes have been shown to play any significant role in hepatic processing of drugs (Estabrook, 1996). These important P450 enzymes generally have broad and overlapping substrate specificity, which poses a serious challenge to the prediction of therapeutic or toxic outcomes of xenobiotic metabolism.

Specific P450 enzyme-substrate recognition interactions have been

This work is supported by National Institutes of Health Grant 1-R43-GM069124-01 "In Silico Assessment of Drug Metabolism and Toxicity".

Article, publication date, and citation information can be found at <http://dmd.aspetjournals.org>.

doi:10.1124/dmd.104.000364.

**ABBREVIATIONS:** QSMR, quantitative structure-metabolism relationship; P450, cytochrome P450; NLM, nonlinear mapping; LOO, leave-one-out; SC, sensitivity coefficient.

studied extensively, including several QSAR and pharmacophore models that have been built and analyzed in reviews (Smith et al., 1997a,b; Lewis et al., 1998, 2002; de Groot et al., 1999; Lewis, 2000; Szklarz et al., 2000; Ekins et al., 2001; de Groot and Ekins, 2002). Electronic models for P450-mediated metabolism have been produced (Jones et al., 2002; Jones and Korzekwa, 1996), which have combined aliphatic and aromatic oxidation reactions to generate predictions for regioselectivities. More recently, this approach has been used to identify the major sites of human CYP3A4 metabolism (Singh et al., 2003). Although useful and thoughtfully designed, these various models used above have limitations, as they were generated with small sets of molecules for a selection of P450s. In contrast, another approach that can be taken is to carefully collate a large amount of substrate-product reactions for human P450s and then categorize the metabolic reactions according to the particular type of chemical transformation [e.g., *N*-dealkylation, *O*-dealkylation, and sulfur (II) oxidation] (Korolev et al., 2003). Recently, we have developed computational algorithms for assessment of the general probability of P450-mediated transformation for drug-like compounds (Korolev et al., 2003) and for prediction of the  $K_m$  of drugs to the active sites of P450 enzymes using this data base (Balakin et al., 2004).

In the present study we have evaluated the possibility of more accurately predicting the rates of P450-mediated metabolic *N*-dealkylation reactions. The work focuses in particular on *N*-dealkylation mediated by two of the clinically relevant human P450 enzymes, CYP3A4 and CYP2D6. These models should serve as a starting point for the development of an integrated automated system for the prediction of metabolic and toxic effects of organic compounds in humans (Bugrim et al., 2004).

### Materials and Methods

**Data Bases.** A total of 83 metabolic *N*-dealkylation reactions with experimental  $\log V_{max}$  values for two major human P450s, CYP3A4 and CYP2D6, were studied in this work (Table 1). Together, both P450s are responsible for hepatic metabolism of ca. 80% of drugs in humans (Yan and Caldwell, 2001). For each reaction, structures of initial substrates and products were obtained from the MetaDrug data base (GeneGo, St. Joseph, MI). These *N*-dealkylation reactions in human enzyme assays generally followed Michaelis-Menten kinetics allowing calculation of  $V_{max}$  values, which ranged from  $1 \times 10^{-6}$  to  $3.3 \times 10^3$  pmol/min/pmol of enzyme.

To clean the input data for their subsequent use in QSAR modeling, we performed an analysis of the initial training data set obtained from the MetaDrug data base. The analysis is based on Sammon nonlinear mapping (NLM) (Sammon, 1969) of the initial substrates' property space. NLM is an advanced multivariate statistical technique that approximates local geometric relationships on a two- or three-dimensional plot. Sammon maps have previously been used for the visualization of protein sequence relationships in two dimensions and comparisons between large compound collections, represented by a set of molecular descriptors (Agrafiotis and Lobanov, 1997; Agrafiotis et al., 1999). In this work, we used NLM for analysis of heterogeneity of the initial data set of *N*-dealkylation reaction substrates. Five molecular descriptors, molecular weight, logarithm of 1-octanol/water partition coefficient ( $\log P$ ), the number of H-bond donors and acceptors, and the number of rotatable bonds were calculated for the entire initial data set of CYP3A4 and CYP2D6 substrates. These descriptors encode the most significant molecular features, such as molecular size, lipophilicity, H-bonding capacity, and flexibility, and are commonly associated with molecular properties determining drug-likeness of small molecule compounds. The Sammon NLM procedure allows the creation of a 2-D image of the studied five-dimensional property space.

The Sammon map generation was conducted using a program developed internally at Chemical Diversity Labs as part of the ChemoSoft™ software suite (Chemical Diversity Labs, Inc. San Diego, CA.). The nonlinear map was built based on the following parameters: maximal number of iterations 300, optimization step 0.3; Euclidean distance was used as a similarity measure.

After the outliers were removed with this technique, we obtained two sets

TABLE 1

List of compounds with  $\log V_{max}$  values for the enzymatic *N*-dealkylation reactions

Data are from the MetaDrug data base (GeneGo, St. Joseph, MI).

Compound	Log $V_{max}$	
	CYP3A4	CYP2D6
Acetylmethadol	1.56	
Alvameline*	-6; -1.30	
Amidopyrine		-0.55
Amiodarone	0.41	
Amodiaquine		-0.70
Azelastine	0.88	0.36
Benzphetamine	1.08	
Caffeine		-2.11
(-)-Cisapride		-6.00
(+)-Cisapride	-0.25	-6.00
(S)-Citalopram		-3.65
Clozapine	0.17	0.79
Dextromethorphan		0.70
Diazepam	0.35	-6.00
Diltiazem	1.00	
diMMAMC [ <i>N,N</i> -dimethyl 7-methoxy-4-(aminomethyl)-coumarin]		-6.00
( <i>R</i> )-Disopyramide	-0.96	-2.30
( <i>S</i> )-Disopyramide	-0.57	-2.30
Ebastine	-0.55	-6.00
EMAMC [ <i>N</i> -ethyl 7-hydroxy-4-(aminomethyl)-coumarin]		-6.00
( <i>R</i> )-Fluoxetine	1.03	
Imipramine	0.38	1.15
K11777 ( <i>N</i> -methyl-piperazine-Phe-homoPhe-vinylsulfonyl-benzene)	1.02	
( <i>R</i> )-Ketamine		0.34
Lidocaine	2.40	
Lilopristone		-6.00
( <i>S</i> )-Mephobarbital		-6.00
( <i>S</i> )-Methamphetamine		-0.02
Metoclopramide	-1.01	
MHAMC [ <i>N</i> -methyl 7-hydroxy-4-(aminomethyl)-coumarin]		-6.00
Mifepristone	1.56	
Mirtazapine	1.04	0.01
MMAMC [ <i>N</i> -methyl 7-methoxy-4-(aminomethyl)-coumarin]		-6.00
MMPyrC [7-methoxy-4-(methylpyridinium)-coumarin]		-6.00
<i>N</i> -Demethyl-acetylmethadol	1.04	
<i>N</i> -Desmethyl-tramadol	-1.56	
<i>N</i> -Ethyl 7-methoxy-4-(aminomethyl)-coumarin		-6.00
Nortriptyline	0.79	-0.49
Onapristone		-6.00
PHAMC [ <i>N</i> -propyl 7-hydroxy-4-(aminomethyl)-coumarin]		-6.00
Pimozide	0.65	-6.00
PMAMC [ <i>N</i> -propyl 7-methoxy-4-(aminomethyl)-coumarin]		-6.00
Sertraline	-0.24	-0.10
Theophylline	-2.04	-2.09
Tolterodine	0.17	-6.00
Tramadol	0.18	-0.82
Verapamil*	3.52; 3.29	-6.00
Zopiclone	-1.30	-0.70

\* The molecules with two different *N*-dealkylation sites.

of metabolic *N*-dealkylation reactions mediated by CYP3A4 and CYP2D6 enzymes (Table 1). Twenty one molecules are common between these two enzymes, but are characterized with different  $\log V_{max}$  values. The substrates are listed in Table 1 with their  $\log V_{max}$  values for the corresponding CYP3A4- and CYP2D6-mediated reactions.

**Neural Network Modeling.** The NeuroSolution 4.0 program (NeuroDimension, Inc. Gainesville, FL.) was used for all neural network operations. Unless otherwise stated, the modular neural networks with two hidden layers were generated. Modular feed-forward networks are a special class of multilayer perceptrons. These networks process their input using several parallel multilayer perceptrons, and then recombine the results. This action tends to



TABLE 2

The 24-descriptor set selected from 120 initial descriptors by the sensitivity analysis (CYP3A4 *N*-dealkylation set)

Descriptor	Definition	Average SC
C_Density	Density (cleaved fragment)	1.68
A_WPSA-2	Surface-weighted charged partial surface area	1.62
B_HBA	Number of H-bond acceptors	1.54
B_Shadow-X	Surface area projection on <i>X</i> -axis	1.49
B_Zagreb	Sum of the squares of vertex valencies (centroid)	1.49
B_Density	Density (centroid)	1.32
A_Zagreb	Sum of the squares of vertex valencies (whole molecule)	1.28
C_WPSA-3	Surface-weighted charged partial surface area	1.24
B_Vm	Molecular volume (centroid)	1.16
B_Area	Molecular surface area	1.13
C_RPSA	Relative polar surface area	1.12
C_Vm	Molecular volume (cleaved fragment)	1.12
A_RNCG	Relative negative charge	1.1
A_DPASA-3	Difference in charged partial surface area	1.09
A_PNSA-1	Partial negative surface area	1.03
A_Vm	Molecular volume (whole molecule)	1.01
A_FPASA-2	Fractional charged partial surface area	0.99
B_PMI	Principal moment of inertia	0.99
A_DPASA-1	Difference in charged partial surface area	0.97
A_PNSA-1	Fractional charged partial surface area	0.94
C_PNSA-3	Partial negative surface area	0.92
C_PPSA-1	Partial positive surface area	0.91
C_Shadow-XZ	Surface area projection on XZ plane	0.90
A_RNCS	Relative negative charge surface area	0.88

carried out a systematic training-testing experiment based on the cross-validation leave-one-out (LOO) procedure to further reduce the number of inputs, more accurately select descriptors, and find the optimal architecture of the modular neural network. The descriptors were sorted according to the average sensitivity coefficient (SC; the standard deviation of each output divided by the standard deviation of the input which was varied to create the output) as shown in Table 2, and several LOO cross-validation cycles were performed with a gradually reduced number of input variables. In the first round, we used the entire 24-descriptor set; in the second round, we removed one descriptor from the end of the sorted list and generated the models using the remaining 23 descriptors, and so on. The models with different numbers of input variables were assessed using the cross-validated correlation coefficient  $q^2$ . Another parameter used for evaluation of the predictive ability of the generated models is  $\sigma$  (eq. 1), originally proposed by So and Karplus (1997).

$$\sigma = \sqrt{\frac{\sum_{i=1}^N (y_{i,\text{obs.}} - y_{i,\text{pred.}})^2}{N - n - 1}} \quad (1)$$

where  $N$  is a number of compounds in the training set,  $n$  is a number of input variables, and  $y_{i,\text{obs.}}$  and  $y_{i,\text{pred.}}$  are observed and cross-validated predicted activity. Using  $\sigma$  as a selection criterion, one can discriminate between models that give similar correlation coefficients but are different in the number of variables ( $n$ ). Thus, a compromise between the quality of the model and the risk of over-fitting the data can be reached. More specifically, when the neural network has too many adjustable weights compared with the number of training data, the network can memorize the training set.

After the relevant descriptors were found (Table 2), an optimal learning algorithm was identified. Several different neural networks were tested using the cross-validation LOO procedure. It should be noted that we also tried to leave larger fractions out, but even in the case of leave-two-out models, the predictive ability of the networks (expressed as  $q^2$ ) appeared to be reduced (data not shown). Different neural network architectures (Table 3) were automatically built as implemented in the NeuroSolution program and assessed using the LOO value. LOO works by leaving one data point out of the training set and giving the remaining instances (31 in the case of the P4503A4 reaction set) to the learning algorithms for training. The process was repeated 32 times so that each example is a part of the test set only once. The LOO procedure

TABLE 3

Comparative analysis of predictive ability for different neural networks (CYP3A4 data set)

Type of Neural Network	Hidden Layers	$q^2$	$r^2$
Generalized feed-forward network	1	78.3	87.5
Generalized feed-forward network	2	73.1	84.7
Multilayer perceptron	1	77.2	88.1
Modular feed-forward network	2	82.0	87.7
Jordan-Elman network	1	78.7	86.2

tests the model's generalization accuracy, whereas training set accuracy tests only the model's ability to memorize. A comparative LOO analysis was conducted on models trained using several different learning algorithms and the entire 24-descriptor set. The resulting values for average training ( $r^2$ ) and cross-validation ( $q^2$ ) coefficients are reported in Table 3. Among the neural networks tested, modular neural networks with 2 hidden layers provided the best predictive ability. This learning algorithm was used in all further experiments.

**Model Testing.** The developed models were validated using two external test sets, which were not used for training. Nine P4503A4-mediated and five P4502D6-mediated *N*-dealkylation reactions with known  $V_{\text{max}}$  values were collected from the literature. After all the necessary molecular descriptors were calculated as described previously, we separately tested the models for P4503A4 and P4502D6 to predict *N*-dealkylation  $V_{\text{max}}$  values.

## Results

**Molecule Selection.** When we tried to model the entire initial data set, the quality of the models generated was low. Therefore we took steps to remove outlier molecules and produce a more homogeneous "local" model. The first Sammon map used for the training set molecule selection is shown in Fig. 2. Most of the compounds (ca. 90%) are located in a compact region of the map as a long, curved island. Outliers are depicted as black circles and exemplified by four arbitrary structures. In a typical case these outliers represent structurally dissimilar, generally nondrug-like compounds. All such compounds were removed from the data set to ensure some degree of homogeneity of properties for the remaining training set selection. Such a process is an important factor for successful QSAR modeling in this case, when a relatively small number of objects with experimental log  $V_{\text{max}}$  values are available.

**Molecule Feature Selection.** The molecular descriptors predominantly selected in this study are related to the whole-molecular level and are related mainly to the family of Jurs descriptors (Stanton and Jurs, 1990). Other selected factors are the hydrogen bonding capacity, molecular geometry, and topological complexity. The significance of these molecular properties in this particular task is in an agreement with previous observations, where similar or closely related molecular features were considered as the key factors affecting the P450 active site binding affinity. The descriptors related to structural types B and C (Fig. 1), such as density, Zagreb index (the measure of topological complexity, branching) and radius of gyration encode the steric hindrance of the reaction center. In addition, they may relate to the ease of expulsion of the leaving group from the active site. These are all key factors affecting the rate of metabolic conversions. In general, it can be concluded that molecular descriptors selected with the use of the described statistical algorithm adequately describe the molecular properties determining metabolic behavior and, in this case, give a reasonable set of factors governing the rates of metabolic *N*-dealkylation.

**Neural Network Architecture Selection.** Along with the number of input variables, the number of hidden units in the neural network architecture is another important parameter, which is closely related to the generalization ability of the neural network. The principal diffi-

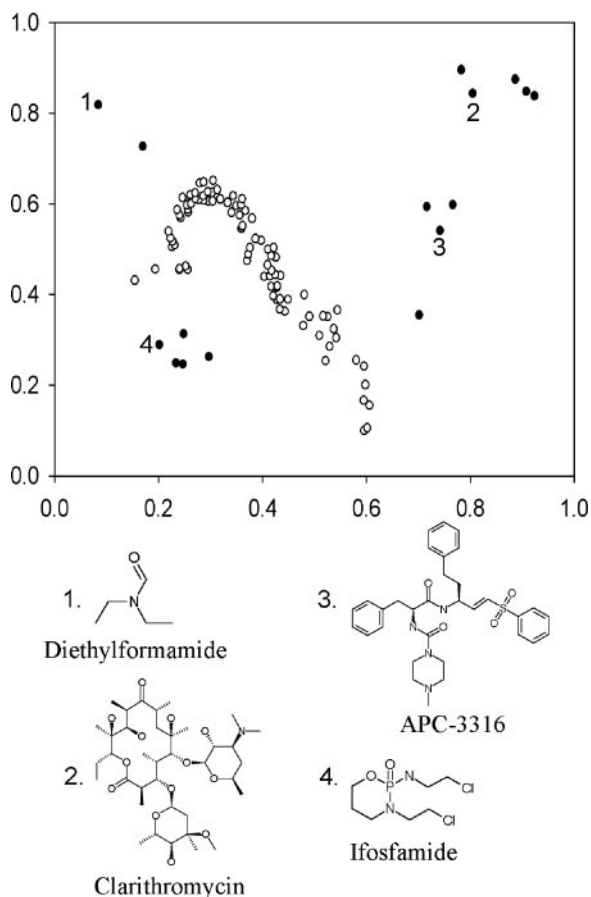


FIG. 2. A Sammon map of the initial data set of substrates of metabolic *N*-dealkylation reactions using five molecular descriptors: molecular weight, logarithm of 1-octanol/water partition coefficient ( $\log P$ ), the number of H-bond donors and acceptors, and the number of rotatable bonds. Structures and names of typical outliers are shown. Only compounds represented by the white circles were used in subsequent QSAR modeling experiments.

culty here is that the optimal architecture depends strongly on the characteristics of the particular problem to be solved, and no a priori recommendations can usually be made to achieve the best predictive ability. To study the influence of the neural network architecture on its predictive ability, LOO cross-validation computations with different numbers of input variables and hidden units were performed. The number of input neurons varied from 5 to 24, and the number of hidden units varied from 2 to 12 (Fig. 3, a and b). The three-dimensional plot of dependence of  $q^2$  on the number of input ( $N$ ) and hidden ( $n$ ) units is shown in Fig. 3a. Thus, the change from 5 to 12 input units brought a meaningful shift in  $q^2$  value from 0.55 to 0.6 to 0.75 to 0.82. This effect leveled off at 12 to 14 descriptors, and then the  $q^2$  did not change significantly upon a further increase of  $N$ . Changing the number of hidden units does not cause such a dramatic change in the fitting performance of the neural network: sinusoidal-like changes in  $q^2$  value were observed upon the increase of  $n$  from 2 to 12, with two maxima at 4 and 10 hidden units. This dependence is most pronounced for a small number of input variables (8–12), whereas for larger  $N$ , the number of hidden units seems to be of low importance for the generalization ability of the neural network. The importance of hidden units for this QSMR model indirectly implies the presence and importance of higher order terms in the QSMR equation modeled by neural network. The three-dimensional plot of the dependence of the parameter  $\sigma$  on the number of input and hidden units (Fig. 3b) allows us to find the optimal solution. For clarity, only

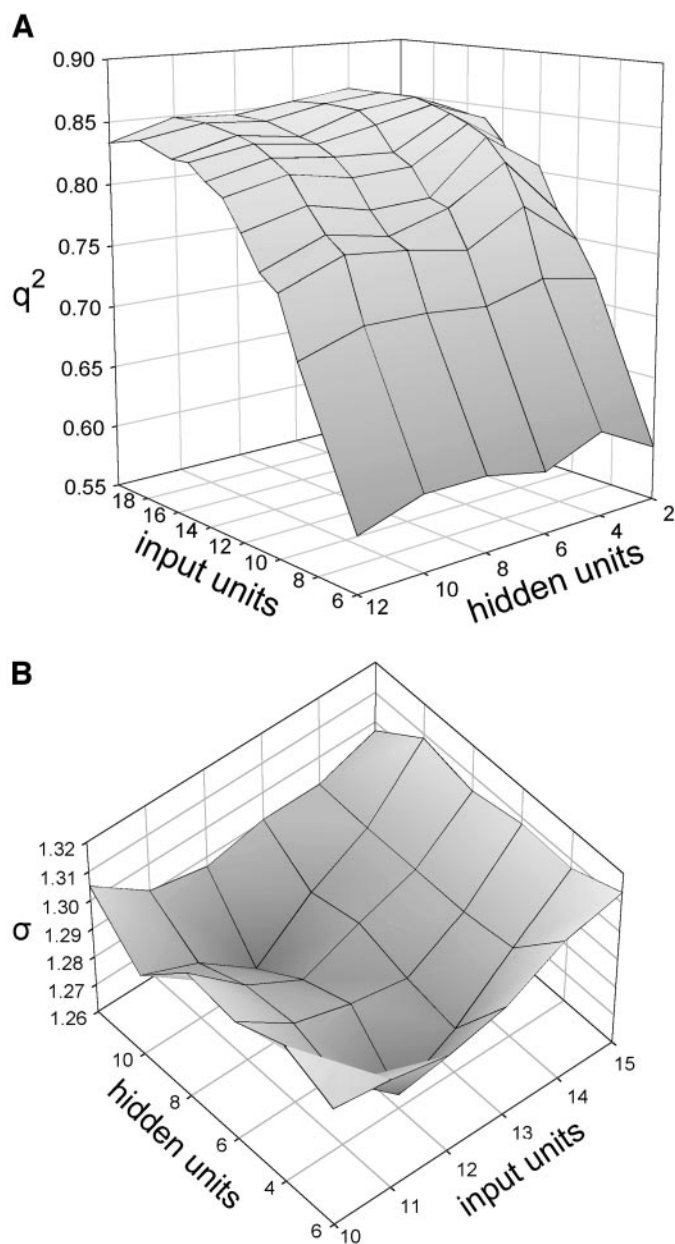


FIG. 3. A, plot of  $q^2$  as a function of the number of input and hidden nodes (CYP3A4 data set). B, plot of  $\sigma$  as a function of the number of input and hidden nodes (CYP3A4 data set).

the area restricted by 10 and 15 input units is shown. There are two local minima on the surface shown here, corresponding to two optimal neural network architectures. The best  $\sigma$  value is achieved for 12 input and 4 hidden units. It is noteworthy that the neural network model using the subset of only 12 inputs provides similar predictive ability as compared with the network developed using 24 input variables. This could be the result of filtering out redundant, or nearly redundant, parameters from the set of independent variables.

The goodness of fit, as judged by the squared correlation coefficient for the training selection,  $r^2$ , can serve as an additional selection criterion for the best model (although there are some limitations to this if the model is over-fitted). The closer this value is to 1, the better the model is. For reasonable regression models,  $q^2$  should be close to  $r^2$ , and is usually smaller (Wold, 1991). Figure 4 shows the dependence of  $q^2$  and average value of  $r^2$  on the number of input variables for

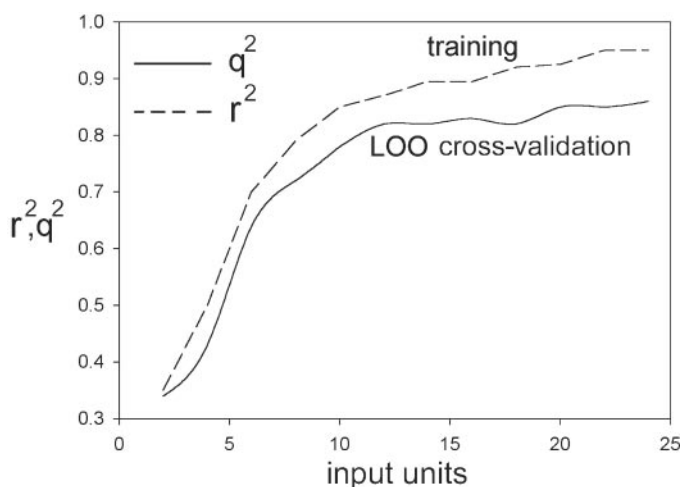


FIG. 4. Variation of  $r^2$  and  $q^2$  as a function of the number of input nodes used in the LOO cross-validation (CYP3A4 data set).

LOO cross-validation experiments using the modular neural network with four hidden units. The observed dependences are similar to each other: the change from 5 to 12 input units causes clear increases in  $r^2$  and  $q^2$  values; the predictive ability and the goodness of fit do not change significantly upon a further increase of  $N$ . It can be generally concluded from the plots shown that for the studied training set, 12 input independent variables (descriptors 1–12 in Table 2) and 4 hidden units make a good compromise between the generalization abilities of the modular neural network and the number of adjustable weights.

**QSMR Modeling the CYP3A4 *N*-Dealkylation Set.** The QSMR models with the lowest  $\sigma$  value were used for further analysis. Figure 5 shows the cross-validated versus observed reaction rates for the best LOO cross-validation experiment. There are no outliers in this model and the overall good conformity between the predicted and observed  $\log V_{\max}$  values resulted in comparable  $r^2$  and  $q^2$  values of 0.85 and 0.82, respectively.

Functional plots are useful tools when analyzing the explicit dependencies between input and output variables in the generated neural network models (So and Karplus, 1997). The functional dependence plot for an independent variable was generated by keeping all but one of the 12 descriptors fixed at a constant value (average value) while scanning the variation of  $\log V_{\max}$  with respect to changes in one descriptor between its mean  $\pm$  standard deviation. We generated such functional dependencies for each of 12 descriptors and each of 31 QSMR models produced in the course of the LOO cross-validation procedure. The averaged data with the standard deviation interval were generated for 31 training/cross-validation cycles. Some interesting conclusions can be drawn from this type of analysis. All 12 descriptors can be divided into two categories according to their observed functional dependencies. The first category comprises six descriptors, for which the relatively stable dependencies between input and output variables were observed in these 31 training-validation cycles. In the second category of the remaining six descriptors, the character of functional dependencies can be altered, sometimes substantially, throughout the models.

For instance, the density of centroids (B\_density; Fig. 6) can serve as a measure of steric hindrance of the reaction site. The negative correlation of this latter descriptor with the CYP3A4-mediated *N*-dealkylation rate is intuitively evident and is in good agreement with experimental observations of medicinal chemists in that molecules with sterically hindered reaction sites are usually poor substrates of

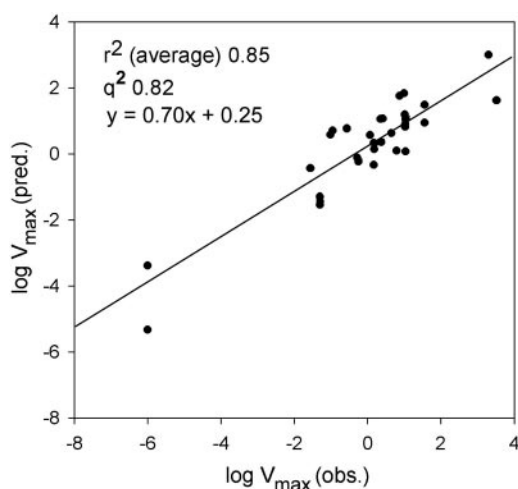


FIG. 5. Plot of the cross-validated  $\log V_{\max}$  (CYP3A4 set, 31 compounds) against the experimental values for the best neural network architecture (modular neural network with 12 input neurons and 2 hidden layers with 4 processing elements).

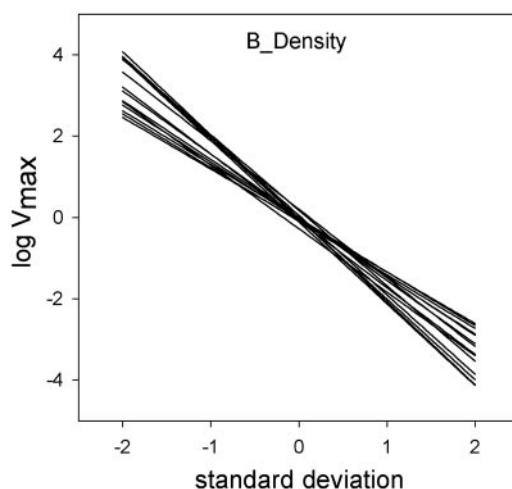


FIG. 6. Functional dependence plots for the descriptor belonging to the "stable" category.

enzymatic reactions (Buchwald, 2001). Figure 7 illustrates this well using two examples from our reference set. (*R*)-Fluoxetine possesses a low-density, sterically unhindered reaction site that is a rapidly metabolized CYP3A4 substrate (Margolis et al., 2000) compared with the sterically hindered mephobarbital. By contrast, disopyramide with its bulky *N*-substituents can be characterized by a relatively low *N*-dealkylation rate (Echizen et al., 2000). Five other "stable" descriptors are related to the family of Jurs charged partial surface area parameters (Stanton and Jurs, 1990). These descriptors encode hybrid electronic and geometric information and capture the ability of the molecule to form hydrogen bonds. It seems these descriptors are important for selective substrate-enzyme interactions in the CYP3A4 active site. However, it should be noted that such discussion of one-dimensional sections through multidimensional surfaces is often only qualitative, whereas quantitative prediction of the metabolic reaction rates requires application of the neural network trained with the relevant input descriptors.

Each of the 12 descriptors used was left out of the set of input variables, and the remaining descriptors were provided to the learning algorithm for training. Figure 8 shows the calculated  $r^2$  and  $q^2$  values obtained in the course of the LOO cross-validation experiment with the reduced set of 11 input variables. One can see that, whereas the

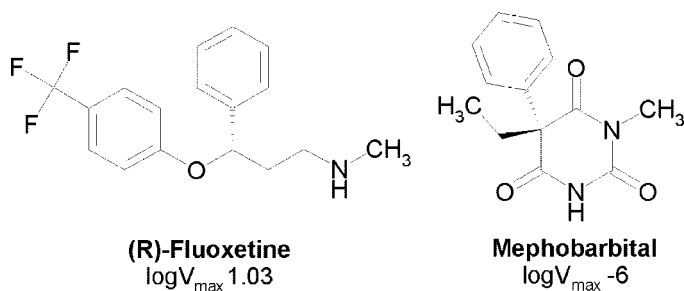


FIG. 7. The influence of steric hindrance of the *N*-dealkylation site upon the reaction rate, showing examples of rapidly and slowly metabolized molecules.

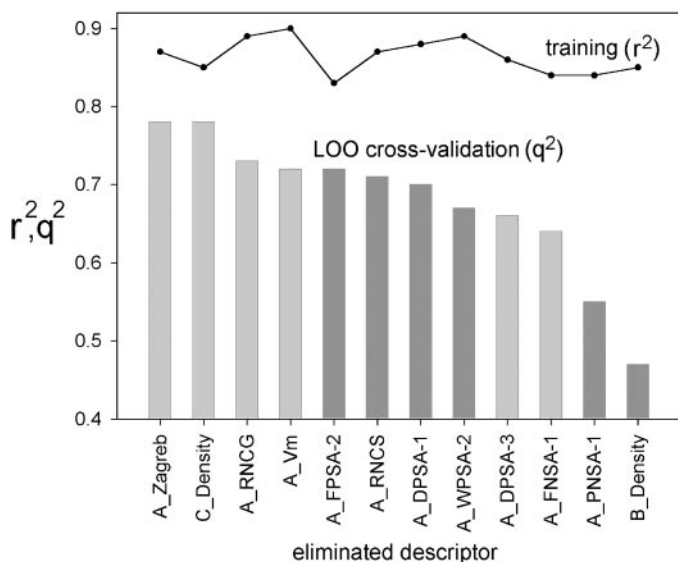


FIG. 8. A plot of the influence of removing one descriptor on the predictive ability ( $q^2$ ) and the average goodness of fit ( $r^2$ ) following LOO cross-validation.

training set correlation goodness of fit ( $r^2$ ) is almost unaffected, the predictive ability of the models is very sensitive to the type and nature of the input variable removed. The most significant reduction in predictive ability is obtained after removal of B\_density and A\_PNSA-1. Both descriptors belong to the first category, and the observed results are in full agreement with their importance noted above for metabolic *N*-dealkylation modeling. At the same time, removal of descriptors with an unstable functional dependence, such as A\_DPSA-3 and A\_FNSA-1, can also result in a substantial reduction of predictive ability (0.63–0.65  $q^2$  values) as compared with the models based on the entire 12-descriptor set. An effect similar to this was observed in another enzyme system (Andrea and Kalayeh, 1991; So and Richards, 1992).

**Comparison of Descriptors Calculated for Different Substrate Elements.** In this work, we have used descriptors derived from three different elements of the substrate's organization (Fig. 1): whole molecule (type A), topological centroid with  $r = 3$  (type B), and leaving fragment (type C). The direct comparison based on calculated squared cross-validation correlation coefficients  $q^2$  is problematic here due to insufficient numbers of descriptors available for type B and C fragments. Therefore, to evaluate their relative importance in the development of predictive QSMR models, we compared the average sensitivity coefficients for descriptors belonging to each particular category. For the entire 24-descriptor set (Table 2) selected by the sensitivity analysis, we conducted a LOO cross-validation experiment and determined the sensitivity coefficients for each descriptor. Then, we calculated the average sensitivity coefficients for each

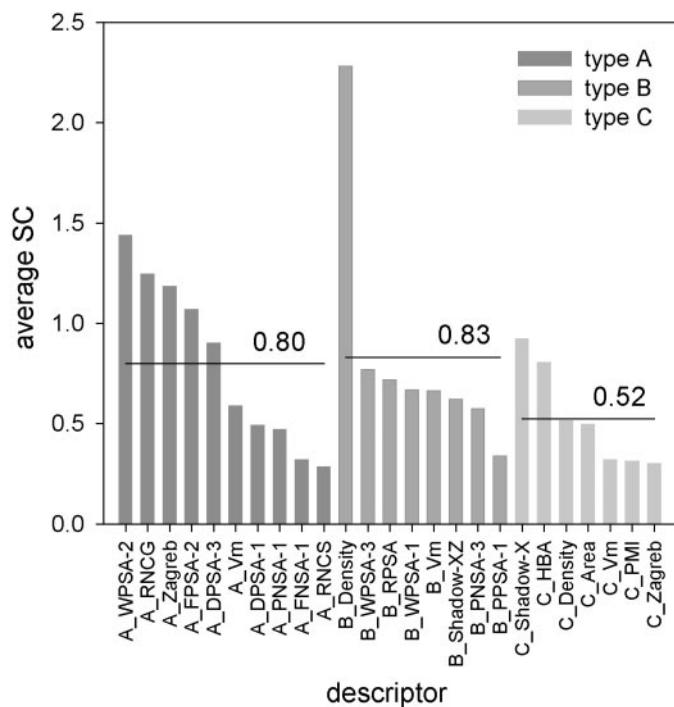


FIG. 9. The relative importance of descriptors derived from three different elements of the substrate organization as measured by the SC.

descriptor category based on these 31 runs (Fig. 9). It appears that the whole-molecular descriptors and topological centroids have the largest average SCs (0.80 and 0.83, correspondingly), followed by the leaving fragments (0.52). Such estimations, though based on indirect data, give a valuable insight into the nature of factors affecting the rates of metabolic *N*-dealkylation reactions.

**QSMR Models for CYP2D6 *N*-Dealkylation Set.** From the extensive QSMR studies described above, we have determined a set of molecular features responsible for *N*-dealkylation rates. It can be assumed that this set of molecular features should be able to model the

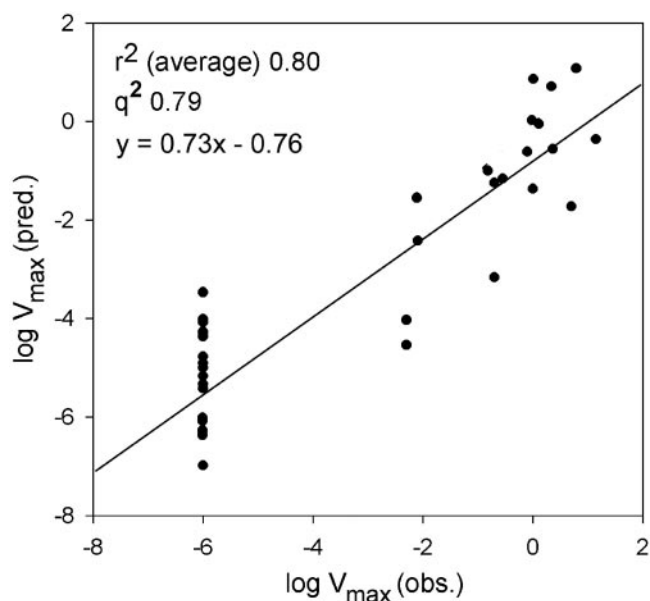
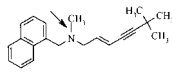
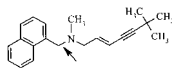
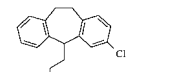
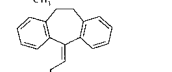
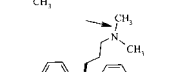
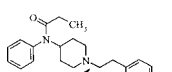
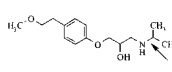
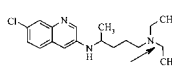
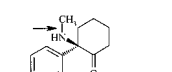
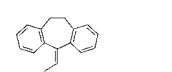
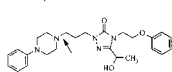
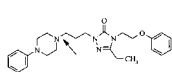
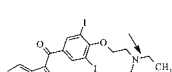
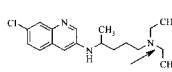


FIG. 10. A plot of the cross-validated log  $V_{\max}$  (CYP2D6 set, 36 compounds) against the experimental values for the best neural network architecture (a modular neural network with 12 input neurons and 2 hidden layers with 4 processing elements).

TABLE 4  
Validation of the models using an external test set

Number	Structure*	Name	P450 Enzyme	Log $V_m$		Reference
				Exp.	Pred.	
				<i>pmol/min/pmol of enzyme</i>		
1		Terbinafine	3A4	0.18	0.05	Vickers et al. (1999)
2		Terbinafine	3A4	0.83	0.44	Vickers et al. (1999)
3		Clomipramine	3A4	-0.37	-1.96	Nielsen et al. (1996)
4		Amitriptyline	3A4	0.49	0.49	Venkatakrishnan et al. (2001)
5		(S)-Citalopram	3A4	-0.15	0.46	Rochat et al. (1997)
6		Fentanyl	3A4	0.59	0.46	Feierman and Lasker (1996)
7		Metoprolol	3A4	-6.00	-5.53	McGinnity et al. (2000)
8		Propafenone	3A4	0.47	0.50	Projean et al. (2003)
9		(R)-Ketamine	3A4	1.71	0.66	Yanagihara et al. (2001)
10		Amitriptyline	2D6	0.17	0.70	Venkatakrishnan et al. (2001)
11		Hydroxynefazodone	2D6	-6.00	-6.32	Rotzinger and Baker (2002)
12		Nefazodone	2D6	-6.00	-5.95	Rotzinger and Baker (2002)
13		Amiodarone	2D6	0.34	0.59	Ohyama et al. (2000)
14		Propafenone	2D6	0.32	-1.30	Projean et al. (2003)

\* Arrow indicates the site of metabolic N-dealkylation.

rates of *N*-dealkylation reactions mediated by other P450s different from CYP3A4. In addition, from a practical point of view, the development of an automated program for prediction of metabolic reaction rates for different enzymes would ideally require the application of a unified set of descriptors for metabolic reactions belonging to one particular chemical type. The CYP2D6 enzyme represents another important member of the P450 superfamily responsible for hepatic metabolism of ca. 30% of drugs (Yan et al., 2004). For QSMR modeling of CYP2D6-mediated *N*-dealkylation reactions (Table 1), we used the same 12-descriptor set as generated and used for CYP3A4 *N*-dealkylation (Fig. 8).

For this CYP2D6 training set, we performed a LOO procedure, which generated 36 QSMR models. Figure 10 shows the cross-validated versus observed  $\log V_{\max}$  values for this model. This plot demonstrates good prediction quality with good  $q^2$  and  $r^2$  values (0.79 and 0.80, correspondingly). The general conclusion that emerges from this experiment is that for the CYP2D6 *N*-dealkylation reaction set, the developed QSMR models based on the same 12 molecular descriptors as for CYP3A4 *N*-dealkylation provide reasonable generalization accuracy and predictive power.

**Test Sets for CYP3A4 and CYP2D6.** There are several ways to evaluate the predictive ability of a computational model; leaving groups out and scrambling the descriptors with the biological activity are perhaps the most widely used. The most valuable test is an external set of molecules that have been excluded from the model-building process (Ekins, 2003). In this study, nine CYP3A4-mediated and five CYP2D6-mediated *N*-dealkylation reactions with known  $V_{\max}$  values were collected from the literature and used to test the respective models. A comparison of the calculated and experimental data for the test set reactions (Table 4) demonstrates a good predictive power of the developed models with  $R^2$  values equal to 0.90 and 0.94 for CYP3A4 and CYP2D6, respectively.

## Discussion

In this study, we have described a neural network QSMR analysis of metabolic *N*-dealkylation reaction rates for two major P450s, CYP3A4 and CYP2D6. This work is a continuation of numerous studies in the field of development of computational models for these P450s (Smith et al., 1997a,b; Lewis et al., 1998; de Groot et al., 1999; Korolev et al., 2003; Balakin et al., 2004; Szklarz et al., 2000; Ekins et al., 2001, 2003; de Groot and Ekins, 2002). To be an effective P450 substrate, molecules should possess a definite avidity to the active sites of P450 enzymes. Upon binding, the molecule can interact either with the heme prosthetic group or with the other regions of the active site. The intermolecular interactions involving polypeptide chains, such as hydrophobic and electrostatic interactions, van der Waals forces, and H-bond formation, are important for binding. The specific microenvironment of the active site of a particular P450 isoform determines the molecular features that a molecule should possess to effectively bind to that site. One of the main conclusions of this study is the requirement for a rigorous appraisal of the properties of a molecule as a whole (structural type A), rather than just relying on knowledge of isolated fragments and functional groups metabolized. In addition, our data indicate the significance of considering properties of topological centroids (type B), which encode the steric hindrance of the reaction site. Based on our calculations, the nature of leaving fragments (type C) is less important for CYP3A4 and is perhaps due to the proposed large volume and complexity of the active site(s) (Ekins et al., 2003). Nevertheless, the complete removal of descriptors belonging to this fragment type leads to a definite reduction of the predictive ability (Fig. 9). As shown by an extensive statistical experiment with diverse architectures of the neural network,

the modular neural network with 12 input neurons and 2 hidden layers with 4 processing elements is an appropriate choice for the cases studied. Robust quantitative dependencies were found in these models, which incorporate higher order terms in the QSMR equation.

In summary, we have demonstrated the feasibility of constructing QSMR models for predicting the approximate human P450-mediated *N*-dealkylation rates of prospective new medicinal agents. The models, developed from the available human metabolism data for CYP3A4 and CYP2D6, performed well, and good regression statistics were achieved, despite the inherent complexity of the systems involved. Using an external test set of molecules not included in the models for both enzymes, we were able to show good correlations ( $R^2$  values equal to 0.90 and 0.94 for CYP3A4 and CYP2D6, respectively) between the experimental and predicted  $V_{\max}$  values. These neural network models can be readily used for scoring drug-like compounds in drug discovery projects, assuming their molecular descriptors are within the range of these current models.

The limitations of the developed models are related to the experimental measurement of metabolism-related parameters, which are inherently prone to errors. For instance, kinetic constants for the same compound vary substantially between studies, depending on the enzyme's source (recombinant P450s, human liver microsomes). In some cases, the reported  $V_{\max}$  values for the same compound can vary by 2 to 3 orders of magnitude, which can seriously impact regression-based QSMR modeling. We obviously cannot expect that the QSMR models based on such small training sets as described in these studies will be predictive for all available compounds that could be used for future testing. The refinement of the models is certainly possible with the availability and incorporation of more compound metabolism data. Future work in expanding the models is underway, alongside the investigation of other algorithms and descriptors for building P450 QSMR models. The latter is important since, presently, descriptors calculated for each enantiomer will be identical; hence pharmacophore-type approaches may be useful for differentiation between each isomer (Ekins et al., 2001).

The overall methodology described here can be extended to the analysis of other types of metabolic transformations (such as *O*-dealkylation) and includes the following steps: 1) dissection of a substrate molecule into the topological centroid of the reaction site and the leaving fragment, 2) calculation of a specific set of descriptors for each element of the substrate's organization, followed by 3) neural network computations. This work illustrates an approach to mining the human P450 metabolism knowledge space using the information from a comprehensive commercially available data base. Further accumulation of experimental data and computational models in this area will pave the way for the development of an integrated and automated system for the prediction of metabolic and toxic effects of organic compounds in humans (Korolev et al., 2003; Balakin et al., 2004; Bugrim et al., 2004). Such an approach incorporates xenobiotic and endobiotic metabolic pathway data bases (along with the routes for regulation of these pathways) together with methods for their reconstruction, representing the application of systems biology (Ekins et al., 2002, 2004). The value of such a software system, incorporating P450 models like those described in this study, will be in the prioritization and selection of molecules for purchase or synthesis in drug discovery, alongside the calculation of other predicted physicochemical properties.

## References

- Agrafiotis DK and Lobanov VS (1997) Nonlinear mapping networks. *J Chem Inf Comput Sci* **40**:1356–1362.
- Agrafiotis DK, Myslik JC, and Salemm FR (1999) Advances in diversity profiling and combinatorial series design. *Mol Divers* **4**:1–22.

- Altomare C, Carrupt PA, Gaillard P, el Tayar N, Testa B, and Carotti A (1992) Quantitative structure-metabolism relationship analyses of MAO-mediated toxication of 1-methyl-4-phenyl-1,2,3,6-tetrahydropyridine and analogues. *Chem Res Toxicol* **5**:366–375.
- Andrea T, and Kalayeh H (1991) Applications of neural networks in quantitative structure-activity relationships of dihydrofolate reductase inhibitors. *J Med Chem* **34**:2824–2836.
- Balaban AT (1982) Highly discriminating distance-based topological index. *Chem Phys Lett* **89**:399–404.
- Balakin KV, Ekins S, Bugrim A, Ivanenkov YA, Korolev D, Nikolsky YV, Skorenko AV, Ivashchenko AA, Savchuk NP, and Nikolskaya T (2004) Kohonen maps for prediction of human cytochrome P450 3A4. *Drug Metab Dispos* **32**:1183–1189.
- Bigus JP (1996) *Data Mining with Neural Networks*. McGraw-Hill, New York.
- Bodor N (1999) Recent advances in retrometabolic design approaches. *J Control Release* **62**:209–222.
- Bollard ME, Holmes E, Blackledge CA, Lindon JC, Wilson ID, and Nicholson JK (1996) <sup>1</sup>H and <sup>19</sup>F-NMR spectroscopic studies on the metabolism and urinary excretion of mono- and disubstituted phenols in the rat. *Xenobiotica* **26**:255–273.
- Bouska JJ, Bell RL, Goodfellow CL, Stewart AO, Brooks CD, and Carter GW (1997) Improving the in vivo duration of 5-Lipoxygenase inhibitors: application of an in vitro glucuronosyl-transferase assay. *Drug Metab Dispos* **25**:1032–1038.
- Buchwald P (2001) Structure-metabolism relationships: steric effects and the enzymatic hydrolysis of carboxylic esters. *Mini Rev Med Chem* **1**:101–111.
- Buchwald P and Bodor N (1999) Quantitative structure-metabolism relationships: steric and nonsteric effects in the enzymatic hydrolysis of noncongener carboxylic esters. *J Med Chem* **42**:5160–5168.
- Bugrim A, Nikolskaya T, and Nikolsky Y (2004) Early prediction of drug metabolism and toxicity: systems biology approach and modeling. *Drug Discov Today* **9**:127–135.
- Cupid BC, Beddell CR, Lindon JC, Wilson ID, and Nicholson JK (1996) Quantitative structure-metabolism relationships for substituted benzoic acids in the rabbit: prediction of urinary excretion of glycine and glucuronide conjugates. *Xenobiotica* **26**:157–176.
- Darvas F (1988) Predicting metabolic pathways by logic programming. *J Mol Graphics* **6**:80–86.
- de Groot MJ, Ackland MJ, Horne VA, Alex AA, and Jones BC (1999) A novel approach to predicting P450 mediated drug metabolism. CYP2D6 catalyzed N-dealkylation reactions and qualitative metabolite predictions using a combined protein and pharmacophore model for CYP2D6. *J Med Chem* **42**:4062–4070.
- de Groot MJ and Ekins S (2002) Pharmacophore modeling of cytochromes P450. *Adv Drug Delivery Rev* **54**:367–383.
- Di Carlo FJ (1990) Structure-activity relationships (SAR) and structure-metabolism relationships (SMR) affecting the teratogenicity of carboxylic acids. *Drug Metab Rev* **22**:411–449.
- Di Carlo FJ, Bickart P, and Auer CM (1986a) Structure-metabolism relationships (SMR) for the prediction of health hazards by the Environmental Protection Agency. I. Background for the practice of predictive toxicology. *Drug Metab Rev* **17**:171–184.
- Di Carlo FJ, Bickart P, and Auer CM (1986b) Structure-metabolism relationships (SMR) for the prediction of health hazards by the Environmental Protection Agency. II. Application to teratogenicity and other toxic effects caused by aliphatic acids. *Drug Metab Rev* **17**:187–220.
- Echizen H, Tanizaki M, Tatsuno J, Chiba K, Berwick T, Tani M, Gonzalez FJ, and Ishizaki T (2000) Identification of CYP3A4 as the enzyme involved in the mono-N-dealkylation of disopyramide enantiomers in humans. *Drug Metab Dispos* **28**:937–944.
- Ekins S (2003) In silico approaches to predicting metabolism, toxicology and beyond. *Biochem Soc Trans* **31**:611–614.
- Ekins S, Boulanger B, Swaan PW, and Hupcey MAZ (2002) Towards a new age of virtual ADMET/TOX and multidimensional drug discovery. *J Comput-Aided Mol Des* **16**:381–401.
- Ekins S, Bugrim A, Nikolsky Y, and Nikolskaya T (2004) Systems biology: applications in drug discovery, in *Drug Discovery Handbook* (Gad S ed) John Wiley & Sons, Inc., New York, in press.
- Ekins S, de Groot M, and Jones JP (2001) Pharmacophore and three-dimensional quantitative structure-activity relationship methods for modeling cytochrome P450 active sites. *Drug Metab Dispos* **29**:936–944.
- Ekins S, Stresser DM, and Williams JA (2003) In vitro and pharmacophore insights into CYP3A enzymes. *Trends Pharmacol Sci* **24**:161–166.
- Eldred DV, Weikel CL, Jurs PC, and Kaiser KLE (1999) Prediction of fathead minnow acute toxicity of organic compounds from molecular structure. *J Med Chem* **12**:670–678.
- Estabrook RW (1996) Cytochrome P450: from a single protein to a family of proteins—with some personal reflections, in *Cytochromes P450: Metabolic and Toxicological Aspects* (Ionnides and Parke eds) pp 4–28, CRC Press, Boca Raton, FL.
- Feierman DE and Lasker JM (1996) Metabolism of fentanyl, a synthetic opioid analgesic, by human liver microsomes. Role of CYP3A4. *Drug Metab Dispos* **24**:932–939.
- Gutman I, Ruscic B, Trinajstić N, and Wilcox CF Jr (1991) Graph theory and molecular orbitals. XII. Acyclic polyenes. *J Chem Phys* **62**:3399–3405.
- Hall LH and Kier LB (1991) The molecular connectivity chi indexes and kappa shape indexes in structure-property modeling. *Rev Comput Chem* **2**:367–422.
- Hayashi S, Watanabe J, and Kawajiri K (1991) Genetic polymorphisms in the 5'-flanking region change transcriptional regulation of the human cytochrome P45011E1 gene. *J Biochem (Tokyo)* **110**:559–565.
- Holmes E, Sweatman BC, Bollard ME, Blackledge CA, Beddell CR, Wilson ID, Lindon JC, and Nicholson JK (1995) Prediction of urinary sulphate and glucuronide conjugate excretion for substituted phenols in the rat using quantitative structure-metabolism relationships. *Xenobiotica* **25**:1269–1281.
- Humphreys WG, Obermeier MT, Barrish JC, Chong S, Marino AM, Murugesan N, Wang-Iverson D, and Morrison RA (2003) Application of structure-metabolism relationships in the identification of a selective endothelin A antagonist BMS-193884 with favourable pharmacokinetic properties. *Xenobiotica* **33**:1109–1123.
- Ionnides C and Parke DV (1996) *Cytochromes P450: Metabolic and Toxicological Aspects*. CRC Press, Boca Raton, FL.
- Jones JP and Korzekwa KR (1996) Predicting the rates and stereoselectivity of reactions mediated by the P450 superfamily. *Methods Enzymol* **272**:326–335.
- Jones JP, Mysinger M, and Korzekwa KR (2002) Computational models for cytochrome P450: a predictive electronic model for aromatic oxidation and hydrogen abstraction. *Drug Metab Dispos* **30**:7–12.
- Kato S, Onda M, Matsukura N, Tokunaga A, Tajiri T, Kim DY, Tsuruta H, Matsuda N, Yamashita K, and Shields PG (1995) Cytochrome P4502E1 (CYP2E1) genetic polymorphism in a case-control study of gastric cancer and liver disease. *Pharmacogenetics* **5**:141–144.
- Korolev D, Balakin KV, Nikolsky Y, Kirillov E, Ivanenkov YA, Savchuk NP, Ivashchenko AA, and Nikolskaya T (2003) Modeling of human cytochrome P450-mediated drug metabolism using unsupervised machine learning approach. *J Med Chem* **46**:3631–3643.
- LeCun Y, Denker JS, Solla SA, and Touretzky D (1990) *Advances in Neural Information Processing Systems*, pp 598–605, Morgan Kaufmann, San Mateo, CA.
- Lewis DF (2000) On the recognition of mammalian microsomal cytochrome P450 substrates and their characteristics: towards the prediction of human p450 substrate specificity and metabolism. *Biochem Pharmacol* **60**:293–306.
- Lewis DF, Modi S, and Dickens M (2002) Structure-activity relationship for human cytochrome P450 substrates and inhibitors. *Drug Metab Rev* **34**:69–82.
- Lewis DFV, Eddershaw PJ, Dickens M, Tarbit MH, and Goldfarb PS (1998) Structural determinants of P450 substrate specificity. *Chem-Biol Interact* **115**:175–199.
- Madsen P, Ling A, Plewe M, Sams CK, Knudsen LB, Sidelmann UG, Ynddal L, Brand CL, Andersen B, Murphy D, et al. (2002) Optimization of alkylidene hydrazide based human glucagon receptor antagonists. Discovery of the highly potent and orally available 3-cyano-4-hydroxybenzoic acid [1-(2,3,5,6-tetramethylbenzyl)-1H-indol-4-ylmethylene]hydrazide. *J Med Chem* **45**:5755–5775.
- Margolis JM, O'Donnell JP, Mankowski DC, Ekins S, and Obach RS (2000) (R)-, (S)-, and racemic fluoxetine are metabolized by multiple human cytochrome P450 enzymes in vitro. *Drug Metab Dispos* **28**:1187–1191.
- McGinnity DF, Parker AJ, Soars M, and Riley RJ (2000) Automated definition of the enzymology of drug oxidation by the major human drug metabolizing cytochrome P450s. *Drug Metab Dispos* **28**:1327–1334.
- Mimoto T, Terashima K, Nojima S, Takaku H, Nakayama M, Shintani M, Yamaoka T, and Hayashi H. (2004) Structure-activity and structure-metabolism relationships of HIV protease inhibitors containing the 3-hydroxy-2-methylbenzoyl-allophenylborstatine structure. *Bioorg Med Chem* **12**:281–293.
- Mulder G (1990) *Conjugation Reactions in Drug Metabolism*. Taylor & Francis, London.
- Nielsen KK, Flinois JP, Beaune P, and Brosten K (1996) The biotransformation of clomipramine in vitro, identification of the cytochrome P450s responsible for the separate metabolic pathways. *J Pharmacol Exp Ther* **277**:1659–1664.
- Ohyama K, Nakajima M, Nakamura S, Shimada N, Yamazaki H, and Yokoi T (2000) A significant role of human cytochrome P450 2C8 in amidarone N-deethylation: an approach to predict the contribution with relative activity factor. *Drug Metab Dispos* **28**:1303–1310.
- Projean D, Baune B, Farinotti JPF, Beaune P, Taburet A-M, and Ducharme J (2003) In vitro metabolism of chloroquine: identification of CYP2C8, CYP3A4, and CYP2D6 as the main isoforms catalyzing N-desethylchloroquine formation. *Drug Metab Dispos* **31**:748–754.
- Rochat B, Amey M, Gillet M, Meyer UA, and Baumann P (1997) Identification of three cytochrome P450 isozymes involved in N-demethylation of citalopram enantiomers in human liver microsomes. *Pharmacogenetics* **7**:1–10.
- Rohrbaugh RH and Jurs PC (1987) Descriptions of molecular shape applied in studies of structure/activity and structure/property relationships. *Anal Chim Acta* **199**:99–109.
- Rotzinger S and Baker GB (2002) Human CYP3A4 and the metabolism of nefazodone and hydroxynefazodone by human liver microsomes and heterologously expressed enzymes. *Eur Neuropsychopharmacol* **12**:91–100.
- Sammon JW (1969) A non-linear mapping for data structure analysis. *IEEE Trans Comp C-18:401–409.*
- Singh SB, Shen LQ, Walker MJ, and Sheridan RP (2003) A model for likely sites of CYP3A4-mediated metabolism on drug-like molecules. *J Med Chem* **46**:1330–1336.
- Smith DA, Ackland MJ, and Jones BC (1997a) Properties of cytochrome P450 isoenzymes and their substrates. Part 1: Active site characteristics. *Drug Discov Today* **2**:406–414.
- Smith DA, Ackland MJ, and Jones BC (1997b) Properties of cytochrome P450 isoenzymes and their substrates. Part 2: properties of cytochrome P450 substrates. *Drug Discov Today* **2**:479–486.
- So SS and Karplus M (1997) Three-dimensional quantitative structure-activity relationships from molecular similarity matrices and genetic neural networks. 2. Applications. *J Med Chem* **40**:4360–4371.
- So SS and Richards WG (1992) Application of neural networks: quantitative structure-activity relationships of the derivatives of 2,4-diamino-5-(substituted-benzyl)pyrimidines as DHFR inhibitors. *J Med Chem* **35**:3201–3207.
- Stanton DT and Jurs PC (1990) Development and use of charged partial surface area structural descriptors in computer-assisted quantitative structure-property relationship studies. *Anal Chem* **62**:2323–2329.
- Szklarz GD, Graham SE, and Paulsen MD (2000) Molecular modeling of mammalian cytochromes P450: application to study enzyme function. *Vitam Horm* **58**:53–87.
- Venkatakrishnan K, von Moltke LL, and Greenblatt DJ (2001) Application of the relative activity factor approach in scaling from heterologously expressed cytochromes P450 to human liver microsomes: studies on amitriptyline as a model substrate. *J Pharmacol Exp Ther* **297**:326–337.
- Vickers AE, Sinclair JR, Zollinger M, Heitz F, Glanzel U, Johanson L, and Fischer V (1999) Multiple cytochrome P-450s involved in the metabolism of terbinafine suggest a limited potential for drug-drug interactions. *Drug Metab Dispos* **27**:1029–1038.
- Wessel MD, Jurs PC, Tolan JW, and Muskal SM (1998) Prediction of human intestinal absorption of drug compounds from molecular structure. *J Chem Inf Comput Sci* **38**:726–735.
- Wiener H (1947) Structural determination of paraffin boiling points. *J Am Chem Soc* **69**:17–20.
- Wold S (1991) Validation of QSARs. *Quant Struct-Act Relat* **10**:191–193.
- Yan Z and Caldwell GW (2001) Metabolism profiling and cytochrome P450 inhibition and induction in drug discovery. *Curr Top Med Chem* **1**:403–425.
- Yanagihara Y, Kariya S, Ohtani M, Uchino K, Aoyama T, Yamamura Y, and Iga T (2001) Involvement of CYP2B6 in N-demethylation of ketamine in human liver microsomes. *Drug Metab Dispos* **29**:887–890.

**Address correspondence to:** Dr. Sean Ekins, Vice President, Computational Biology, GeneGo, 500 Renaissance Drive, Suite 106, St. Joseph, MI 49085. E-mail: sean@gene.com